



HYBRID AUTONOMOUS SYSTEM WITH BACK-TO-BACK POWER CONVERTER AND BATTERY ENERGY STORAGE SYSTEM

Prof. S.T.Gaikwad¹, A.S.Kudalkar²
^{1,2}PVGs COET Pune

Email:suniltgaikwad@rediffmail.com¹, bhasme_amruta@rediffmail.com²

Abstract

Today Power generation from Renewable energy sources like hydro, solar, wind etc. are predominant. In this work hydro, solar and wind energy sources are used for power generation in isolated mode. Two systems are developed Wind-hydro hybrid system and solar hydro hybrid system which are not connected to grid. Squirrel Cage Induction Generator's (SCIG) are used for variable wind power generation and constant hydro power generation. Two back-to-back converters are used in system one on source side and other on load side and in between both converters a battery energy storage system (BESS) is connected which helps for load leveling. A proposed control algorithm for wind side converter is to supply requisite magnetizing current to wind generator and to achieve maximum power tracking (MPT) and for load side converter is to control load voltage and frequency. Perturb and observe method is used for maximum power point tracking (MPPT) in solar generation system. The zigzag transformer is connected near to load to connect its neutral terminal to neutral terminal of load and for filtering zero-sequence components of the load currents. System is modeled in MATLAB by using Sim power system block set. The performance of proposed systems are observed for balanced and unbalance load to observe its capability of voltage and frequency control, load balancing and MPT.

Index Terms: Battery energy storage system (BESS), maximum power tracking (MPT), squirrel cage induction generator (SCIG), Maximum power point tracking (MPPT)

I. INTRODUCTION

In worldwide now a days renewable energy sources are center point for energy production. This is because of increasing prices of fossil fuels. Solar, wind, small hydro and geothermal are natural and easily available sources and inexhaustible in nature. The ability of isolated system using natural energy sources depends on control and stimulation measures. No money is required for using these sources. Another benefit of using renewable energy sources is increasing security of energy supply and no use of fossil fuel means no pollution.

One drawback of using renewable energy sources is they are not continuously available. To overcome the problem of uncertainty sources can combined to get hybrid generation system. Also energy storage systems are used for continuity of supply [1][2]. In some cases Storage is combined with standing reserve from conventional generation to maintain power balance [3]. Stored power is used when generation is less than load and power is stored in storage device when generation is greater than load. Wind and hydro have ability to complement each other [4]. In wind and microhydro generation use of squirrel cage induction generation is explained in [6]-[20], [25].

Solar generation system is combination of PV array and dc-dc converter with MPPT control, PV array consists of modules in which cells are connected. Use of perturb and observe method for MPPT is given in [22]. combination of PV and Hydro is given in [30][31].

In hydro power plant power is generated from the movement of water ie kinetic energy of waterfall is converted in electrical energy. For flow of water it is stored at height called head. Due to pressure of of water flow on turbine blades it rotates shaft. The rotating movement transferred through a shaft to an electric generator which converts mechanical energy of motion of shaft to electrical energy. Power in water depends on vertical distance [i.e., head] and amount of water flow in unit time[i.e., discharge]. SCIG is used in power generation as it is low cost, simple, maintenance free, absence of dc brushless etc[6],[8]. When SCIG is used for power generation reactive power is supplied by capacitor bank connected to its stator terminals.

Wind turbine generators are of two types constant or fixed speed machines and variable speed machines. Constant speed machines rotate at constant speed what may be wind speed. For changing wind speeds efficiency is less for fixed speed wind turbine. In variable speed wind turbine machine rotational speed varies in accordance with wind speed. This variable wind turbine has advantages like increased efficiency, reduced mechanical stress, improved power quality and dynamically compensate for torque and power pulsation. The grid connected variable wind speed power generation system based on SCIG use back-to- back connected power converters. In such case power converter decouples the SCIG from the grid resulting in improved reliability.

The system applied in this work is three-phase four wire isolated (autonomous) wind hydro hybrid system. System is not connected to grid as isolated so it can be applied to place where wind and hydro source exists at a time. Eg. Andaman and Nicobar group of islands [26]. In this system two squirrel cage induction generators are used one is used for variable speed wind turbine denoted as SCIG_w and another is for constant speed/power hydro turbine denoted as SCIG_h. Suffix w is used for wind turbine and suffix h is used for hydro turbine.

Schematic diagram of wind-hydro hybrid system is shown in fig.1. Schematic diagram of solar-hydro system is same only wind generation

is replaced by solar generation. Two converters are connected back- to- back. Both are pulse width modulation controlled [PWM] insulated-gate-bipolar-transistors [IGBT]. First converter is connected to stator terminals of SCIG_w called as machine side converter and second is connected to stator terminals of SCIG_h that is hydro machine called load side converter as load is connected near this converter. Power flow is bidirectional in system due to back-to-back converter connection.

For the function of load leveling that is when wind is less or load is variable battery energy storage system [BESS] is used. BESS is connected in between two converters we can call it as dc bus and due to such connection no additional converter is require for battery connection. BESS also keeps dc bus voltage constant during variable loads. Inductor is connected in series with battery to filter ripple in battery current.

The zig-zag transformer is connected near to load. The neutral point of transformer is connected to neutral point of load. This transformer has three single phase windings with 1:1 turns ratio. It is connected parallel to load for filtering zero-sequence components of load current and also its winding trap triplen harmonics (third, ninth, fifteenth, etc).

This hybrid system works on new control concept which make system to work at maximum power tracking (MPT), control of voltage and frequency ,harmonic elimination, load leveling and load balancing. The function of machine side converter is to supply requisite magnetizing current to SCIG_w and to get MPT. Another converter called as load side converter basically in grid connected system this is called as grid side converter. Actual function of this converter is to keep dc-link voltage constant. But in this system BESS is doing work of maintaining dc-link voltage constant. So work of load side converter is different in this system. It supplies reactive power to the load. For SCIG_h reactive power is given by capacitor bank connected to its stator terminals. Load side converter also balance active power in system by transferring excess power to battery when load is less than power generated and by receiving deficit power from battery when load is greater than power generated.

For load side converter indirect current control is used. Control signals for switching this

converter are generated from error of reference and actual stator currents of hydro generator. Load current and load side converter current is not used thus reducing number of current sensors. As load side current is not used and hydro generator current is used. This control also helps to balance and sinusoidal the SCIG_h currents at nominal frequency. Zig-zag transformer and load side converter does the

compensation of unbalance and harmonics in load current.

Remaining paper sequence is as follows. In section II principle of operation and converter control of hybrid system is given. In section III selection of component ratings is given. Section IV Solar system is explained. In section V MATLAB diagram of two systems are explained. VI Results are discussed VII Conclusion

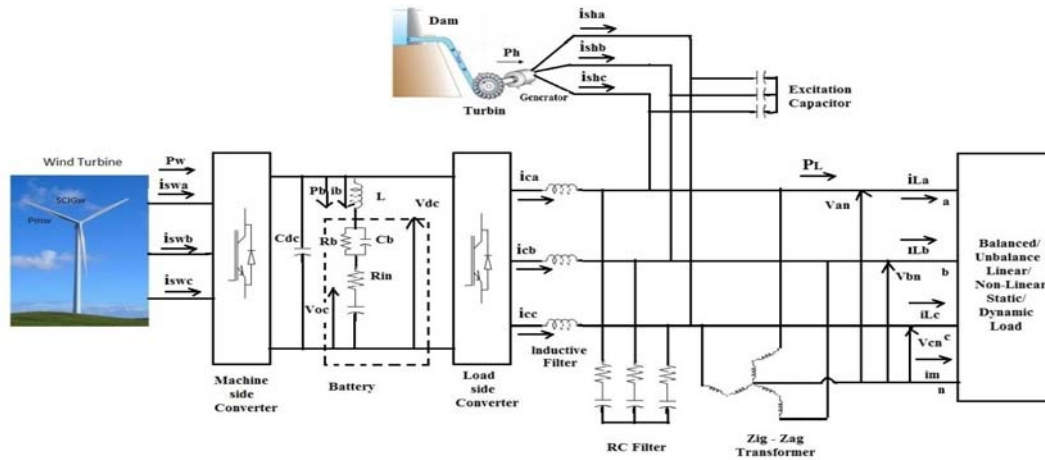


Fig.1. Schematic diagram of wind hydro hybrid system

II. PRINCIPLE OF OPERATION AND CONVERTER CONTROL OF HYBRID SYSTEM

A Principle of Operation

Two converters are connected back-to-back in system. These are PWM controlled IGBT based voltage source converters. One is machine side converter and other is load side converter. The use of machine side converter is to provide requisite magnetizing current to wind generator and use of load side converter is for VFC i.e. voltage and frequency control at load terminals by maintaining active and reactive power balance [1].

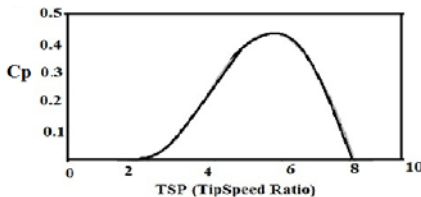


Fig. 2. Coefficient of performance (C_p) versus tip speed ratio (λ) for wind turbine.

Wind generator is operated at optimal tip-speed ratio as in fig.2.to achieve MPT. The tip

speed ratio is ratio of tip speed of blade to the actual wind speed.

$$\lambda = \frac{\text{Tip speed of blade}}{\text{wind speed}}$$

Optimal tip speed ratio is ratio at which maximum power is extract from wind. That means mechanical power generated at this speed lies on the maximum power line of the turbine, as in fig.3.

Machine side converter controller operating principle is based on decoupled control of d-axes and q-axes stator currents of wind generator. The d-axis is along with rotor flux axes as in fig.4. The reference reactive component or d-axes stator current of wind generator is calculated from required magnetizing flux of wind generator. The reference value of q-axes or active component of wind generator stator current is calculated from error between the desired speed and actual rotor speed of wind generator.

Rotor speed set point changes with change in wind speed. The difference between actual rotor

speed and reference rotor speed is calculated. This difference is given as input to controller of machine side converter. This controller is called as speed controller.

The reference value of q-axis stator current of wind generator is calculated as output of speed controller. Reference d-q stator currents of wind generator are converted to three phase currents I_{swa}^* , I_{swb}^* and I_{swc}^* called as reference three phase stator currents of wind generator. These three phase reference currents are compared with actual value of three phase stator currents of wind generator. This calculated difference of current are used to generate control signals for machine side converter.

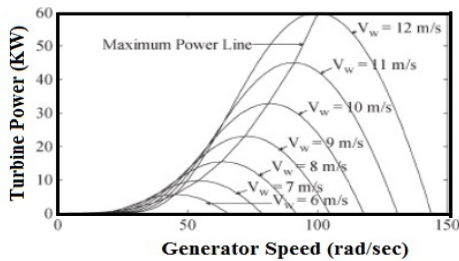


Fig.3. Mechanical power output of wind turbine versus SCIG_w speed for different wind speed

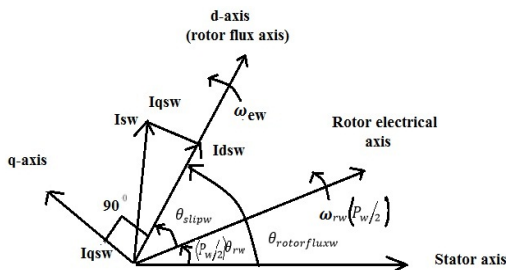


Fig.4. Phasor diagram of rotor flux oriented control of SCIG.

Load voltage magnitude and load frequency care is taken by load side converter and it is controlled for the same purpose. To maintain load frequency constant it is important to transfer surplus active power generated to battery i.e. when load connected to system is less than power generated by system. Also battery must supply deficit in the generated power i.e. when load connected to system is greater than power generated by system. Same way voltage is kept constant in system by reactive power requirement balancing of load. This is done by load side converter. Detailed system of two converters is given as below.

B Control of Machine Side Converter

To achieve optimum torque for MPT and to give required magnetizing current to wind generator are the control aims of machine side converter. Fig.5. shows technique applied for machine side converter [1].

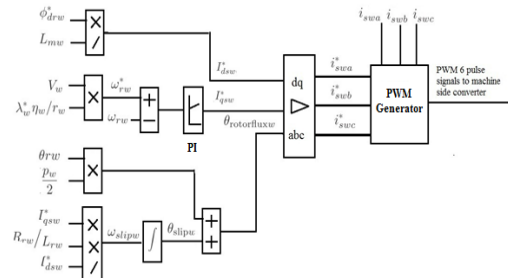


Figure.5. Control scheme of machine-side converter

i) Speed control loop for reference q-axis wind generator stator current generation and for MPT.

In this algorithm wind speed value is given as input and rotor position (θ_{rw}) value is taken from wind generator. Using wind speed V_w , gear ratio η_w , turbine radius r_w and rotor speed the tip speed ratio is calculated from given equation,

$$\lambda_w = \frac{\omega_{rw} r_w}{\eta_w V_w} \tag{1}$$

The wind generator should be operated at optimum tip speed ratio (λ_w^*) for MPT in wind-turbine generation system as in fig 5. By using equation (1) reference rotor speed (ω_{rw}^*) is calculated as,

$$\omega_{rw}^* = \frac{\lambda_w^* V_w \eta_w}{r_w} \tag{2}$$

The actual rotor speed ω_{rw} is compared with this calculated reference rotor speed and rotor speed error (ω_{rwer}) is calculated at nth sampling instant as follows,

$$\omega_{rwer(n)} = \omega_{rw(n)}^* - \omega_{rw(n)} \tag{3}$$

This calculated error of rotor speed is given as input to the speed proportional integral (PI). PI is used in this controller because it continuously calculates an error values as difference between a desired set point and measured process variable and it is required to get solve equation (3) and equation (4) as value of error is calculated at nth sampling instant. Error signal goes into the PI controller where it gets multiplied by proportional and integral constants. At output of speed PI controller reference q-axis wind generator stator current (I_{qsw}^*) is obtain at nth

sampling instant with proportional gain $K_{p\omega}$ and integral gain $K_{i\omega}$. PI controller is called as speed PI as it works on speed error in this control.

$$I_{qs\omega(n)}^* = I_{qs\omega(n-1)} + K_{p\omega}(\omega_{r\omega(n)} - \omega_{r\omega(n-1)}) + K_{i\omega}\omega_{r\omega(n)} \quad (4)$$

ii) Reference d-axis stator current generation for wind generator

Rotor flux set point ($\phi_{dr\omega}^*$) is used to find the reference d-axis wind generator stator current ($I_{ds\omega}^*$) at nth sampling is given as,

$$I_{ds\omega(n)}^* = \frac{\phi_{dr\omega}^*}{L_{m\omega}} \quad (5)$$

Where $L_{m\omega}$ is magnetizing inductance of SCIG.

PWM Signal Generation for Machine Side Converter

Transformation angle $\theta_{rotorfluxw}$ is generated as shown in fig.4. This $\theta_{rotorfluxw}$ is used for generation of three phase reference wind generator stator currents ($I_{s\omega a}^*$, $I_{s\omega b}^*$ and $I_{s\omega c}^*$) using following equation,

$$\theta_{rotorfluxw} = \theta_{slip\omega} + \left(\frac{P_{\omega}}{2}\right)\theta_{r\omega} \quad (6)$$

Where $\theta_{slip\omega}$ is slip angle generated by taking integration of slip frequency $\omega_{slip\omega(n)}$,

$$\theta_{slip\omega(n)} = \int \omega_{slip\omega(n)} dt \quad (7)$$

At nth sampling instant we gate value of $\omega_{slip\omega}$ which is calculated as,

$$\omega_{slip\omega(n)} = \frac{(R_{r\omega} I_{qs\omega(n)}^*)}{(L_{r\omega} I_{ds\omega(n)}^*)} \quad (8)$$

Where,

$L_{r\omega}$ is the rotor self-inductance of wind generator.

$R_{r\omega}$ is the rotor resistance of wind generator.

As explained above transformation angle $\theta_{rotorfluxw}$ is used for d-q to abc transformation. Where wind generators d-q components of stator current ($I_{ds\omega}^*$ and $I_{qs\omega}^*$) are converted to three phase reference wind generator stator currents, ($i_{s\omega a}^*$, $i_{s\omega b}^*$, $i_{s\omega c}^*$) as in equations,

$$i_{s\omega a}^* = I_{ds\omega}^* \sin(\theta_{rotorfluxw}) + I_{qs\omega}^* \cos(\theta_{rotorfluxw}) \quad (9)$$

$$i_{s\omega b}^* = I_{ds\omega}^* \sin(\theta_{rotorfluxw} - \frac{2\pi}{3}) + I_{qs\omega}^* \cos(\theta_{rotorfluxw} - \frac{2\pi}{3}) \quad (10)$$

$$i_{s\omega c}^* = I_{ds\omega}^* \sin(\theta_{rotorfluxw} + \frac{2\pi}{3}) + I_{qs\omega}^* \cos(\theta_{rotorfluxw} + \frac{2\pi}{3}) \quad (11)$$

Actual stator currents $I_{s\omega a}$, $I_{s\omega b}$ and $I_{s\omega c}$ of wind generator are compared with three phase reference currents ($i_{s\omega a}^*$, $i_{s\omega b}^*$, $i_{s\omega c}^*$) to find wind generator stator current errors. These error currents are amplified with gain ($k=5$) and compared with 10kHz fixed frequency triangular carrier wave having unity amplitude. As a result gating signals for machine side converter are generated. 50microseconds sampling time is taken for controller, as this time is sufficient for completion of calculation in typical DSP controller.

C Control of Load Side Converter

To maintain load voltage and frequency constant at load terminal irrespective of connected load is objective of load side converter. For this the power balance in system is must. The power balance in system is done by transferring excess power to battery in case of load requirement is less than generated power and transferring power from battery to load when load requirement is greater than power generated in system. To keep load voltage constant the required reactive power for load is supplied by load side converter. The control signals for switching of the load-side converter are generated from the error of the reference and the actual stator currents of SCIGh. The control algorithm for load side converter control is shown in fig.6.

i) Reference Three Phase Current Generation for Hydro Generator.

The reference voltages V_{an}^* , V_{bn}^* and V_{cn}^* are calculated at time t for load voltage control as,

$$V_{an}^* = \sqrt{2}V_t \sin(2\pi ft) \quad (12)$$

$$V_{bn}^* = \sqrt{2}V_t \sin(2\pi ft - 120^\circ) \quad (13)$$

$$V_{cn}^* = \sqrt{2}V_t \sin(2\pi ft + 120^\circ) \quad (14)$$

Where,

f = nominal frequency as 50Hz,

V_t = rms phase-to-neutral load voltage

consider as 240volts.

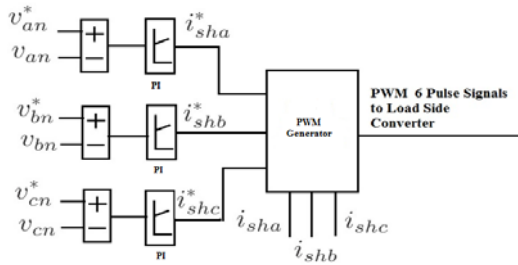


Fig.6. Control scheme of load-side converter

Actual load three phase voltages V_{an} , V_{bn} , V_{cn} are sensed and compared with above calculated reference three phase voltages to get error voltages V_{anerr} , V_{bnerr} , V_{cnerr} at nth sampling instant as in below equations,

$$V_{anerr(n)} = \{V_{an(n)}^* - V_{an(n)}\} \quad (15)$$

$$V_{bnerr(n)} = \{V_{bn(n)}^* - V_{bn(n)}\} \quad (16)$$

$$V_{cnerr(n)} = \{V_{cn(n)}^* - V_{cn(n)}\} \quad (17)$$

These voltage error signals are given as input to PI voltage controller with proportional gain K_{pv} and integral gain K_{iv} to get reference three phase currents of hydro generator as,

$$\begin{aligned} i_{sha(n)}^* &= i_{sha(n-1)} + K_{pv}(V_{anerr(n)} - V_{anerr(n-1)}) \\ &+ K_{iv}V_{anerr(n)} \end{aligned} \quad (18)$$

$$\begin{aligned} i_{shb(n)}^* &= i_{shb(n-1)} \\ &+ K_{pv}(V_{bnerr(n)} - V_{bnerr(n-1)}) \\ &+ K_{iv}V_{bnerr(n)} \end{aligned}$$

$$\begin{aligned} i_{shc(n)}^* &= i_{shc(n-1)} \\ &+ K_{pv}(V_{cnerr(n)} - V_{cnerr(n-1)}) \\ &+ K_{iv}V_{cnerr(n)} \end{aligned} \quad (20)$$

Actual hydro generator stator currents (i_{sha} , i_{shb} , i_{shc}) are compared with reference three phase hydro generator stator currents (i_{sha}^* , i_{shb}^* , i_{shc}^*) to find hydro generator error currents.

$$i_{shaerr} = i_{sha}^* - i_{sha} \quad (21)$$

$$i_{shberr} = i_{shb}^* - i_{shb} \quad (22)$$

$$i_{shcerr} = i_{shc}^* - i_{shc} \quad (23)$$

These current errors are amplified with gain ($k=5$) and compared with 10kHz fixed frequency triangular carrier wave having unity amplitude. As a result gating signals for load side converter are generated. 50microseconds sampling time is taken for controller, as this time is sufficient for completion of calculation in typical DSP controller

III. COMPONENT RATINGS

A) Selection of Wind Turbine and Gear Ratio

While designing Rating of wind turbine is taken as 55 kW at wind speed of 11.2m/s, which is considered as rated wind speed. Below rated wind speed, the mechanical power (P_m) capture by the turbine is function of wind speed (V_w), coefficient of performance (C_p), radius of turbine (r_w) and density of air (ρ) as in below

$$P_m = 0.5C_p\pi r_w^2\rho V_w^3 \quad (24)$$

Fig.2. shows relation between tip speed ratio and coefficient of performance for typical wind turbine. At optimum tip speed ratio (λ_w^*) we get maximum coefficient of performance (C_{pmax}). The values of (λ_w^*) and (C_{pmax}) are find from fig.2.and these are 5.66 and 0.4411 respectively. Let convert equation (5.32) for value of wind turbine radius and substituting values of $C_{pmax} = 0.4411$, $\lambda_w^* = 5.66$, $V_w = 11.2$ m/s, Air density $\rho = 1.1544$ kg/m²we get $r_w = 7.5$ meter as below,

$$r_w = \sqrt{\left[\frac{55000}{\{0.5*0.4411*1.1544*\pi*(11.2^3)\}}\right]} 7.5 \text{ m} \quad (25)$$

The gear ratio is calculated by using equation,

$$\eta_{\omega} = \frac{\omega_{r\omega}r_{\omega}}{\lambda_{\omega}V_{\omega}} \quad (26)$$

Where at 11.2m/s wind speed, generator rotor speed is consider as 100rad/second and substituting radius of wind turbine =7.5m, tip speed ratio =5.66 so we gat value of gear ratio = 12 as in below,

$$\eta_{\omega} = \frac{\omega_{r\omega}r_{\omega}}{\lambda_{\omega}V_{\omega}} = \frac{100*7.5}{5.66*11.2} = 11.811 \cong 12 \text{ (selected)}$$

From equation (27) C_p is the function of tip speed ratio λ and blade-pitch angle β [27] as

$$C_p(\lambda, \beta) = 0.73 \left(\frac{151}{\lambda_i} - 0.002 \cdot \beta - 13.2 \right) e^{-(18.4/\lambda_i)} \quad (27)$$

Where

$$\frac{1}{\lambda_i} = \frac{1}{(\lambda + 0.08\beta)} - \frac{0.035}{\beta^3 + 1} \quad (28)$$

To stimulate wind turbine equations (24) to (28) are used.

The Blade-pitch control is used in real turbine for wind speed above rated wind speed. In case of above rated wind speed turbine blades are pitched slightly out of wind to limit power and when wind speed decreases blades are turned back in to the wind.

B) Battery Design and Voltage Selection for DC Link

For satisfactory PWM control, dc-bus voltage must be more than the peak of the line voltage [29],

$$V_{dc} > \left\{ 2 \sqrt{\frac{2}{3}} V_{ac} \right\} m_a \quad (29)$$

Where,

m_a = modulation index, normally consider 1 with maximum value.

V_{ac} = the rms value of line voltage on ac side of the PWM converter.

DC-link is connected between two converters dc sides and on other sides of two converters are ac sides. From both sides there is a constraint on dc-link by ac-voltages of both converters. Maximum rms value of line voltages at load terminal and wind generator terminal is 415v.Consider above equation (29) and substituting value 415v in it, we get $V_{dc} = 677.7$, but value of V_{dc} is greater than this so considering $V_{dc} = 700v$.

The system ability is consider as to supply for 10 hour load of 60 kW, so storage capacity of battery bank we want to design is 600kwh. Each cell has capacity of 12v in commercially available battery bank. The nominal capacity of each cell is taken as 150A.h. To get 700vdc-bus voltage through series connected cells each of 12v, we must use $700/12= 59$ number of cells in series. Storage capacity of this combination is 150A.h, and total ampere hours required is $(600kW.h/700v)=857A.h$, the number of sets

required to be connected in parallel may be $(857A.h/150A.h)=5.71$ or it is taken as 6. Thus battery bank is made up of 6 parallel- connected sets of 59 series-connected battery cells.

Energy storage capacity of battery is explained using Thevenin's model. In this model resistance (R_b) is connected in parallel with capacitance (C_b). This parallel combination is connected in series with internal resistance (R_{in}) and an ideal voltage source of 700volts is used for modeling battery. Following equation is used to find equivalent capacitance (C_b) as in [21][20],

$$C_b = \frac{(KW.h * 3600 * 1000)}{0.5(V_{ocmax}^2 - V_{ocmin}^2)} \quad (30)$$

Where,

$$kWh=600, V_{ocmax} = 750 V, V_{ocmin} = 680 V$$

Substituting values in above equation we gate $C_b = 43.156F$.

IV. SOLAR SYSTEM

PV panel consist of series and parallel combination of PV modules. The PV array configured by 36 parallel connected PV strings and 5 modules connected in series per string. Number of cells per module is 96. PV panel generation is taken for 1000w/m 2irradiation. Module type used for solar generation is SPR-305-WHT.

V. MATLAB DIAGRAM OF TWO SYSTEMS

Schematic diagram shown in fig.1. is developed in MATLAB using Simulink and Sim Power System set toolboxes. MATLAB diagram of wind-hydro hybrid system is shown in Fig.7. And MATLAB diagram of solar-hydro hybrid system is shown in fig.8.

VI. RESULTS AND DISCUSSION

1. Results for Wind-Hydro hybrid system

Wind-hydro hybrid system performance is observed for parameters such as waveforms of the SCIGw stator current (i_{sw}), SCIGH stator current (i_{sh}), load-side converter current (i_c), three-phase load voltage (v_L), three-phase load current (i_L), single-phase load currents (i_{La} , i_{Lb} , and i_{Lc}), zigzag transformer currents (i_{ta} , i_{tb} , i_{tc} , and i_{tn}), load frequency (f_L), rms value of phase load voltage (V_t), SCIGw stator frequency (f_w), battery current (I_b), battery voltage (V_{dc}), SCIGw stator power (P_w), SCIGH stator power (P_h), load power (P_L), battery power (P_b), coefficient of power (C_p), SCIGw rotor speed (ω_{rw}), and wind velocity (V_w).

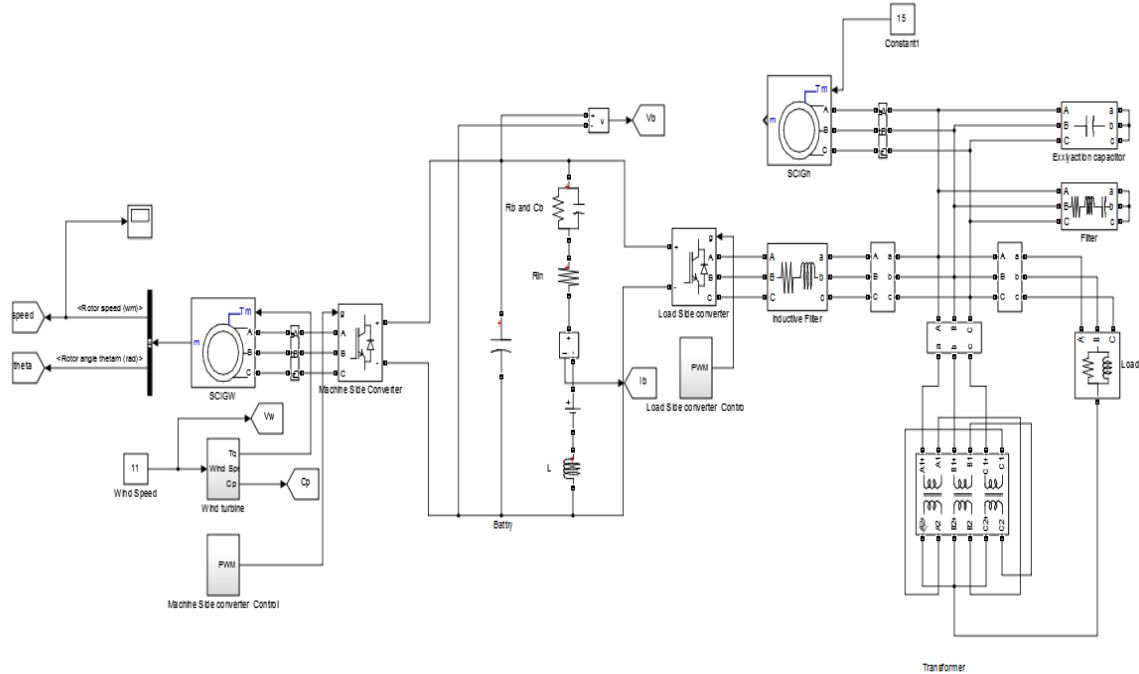


Fig.7. MATLAB simulation diagram of wind-hydro hybrid system.

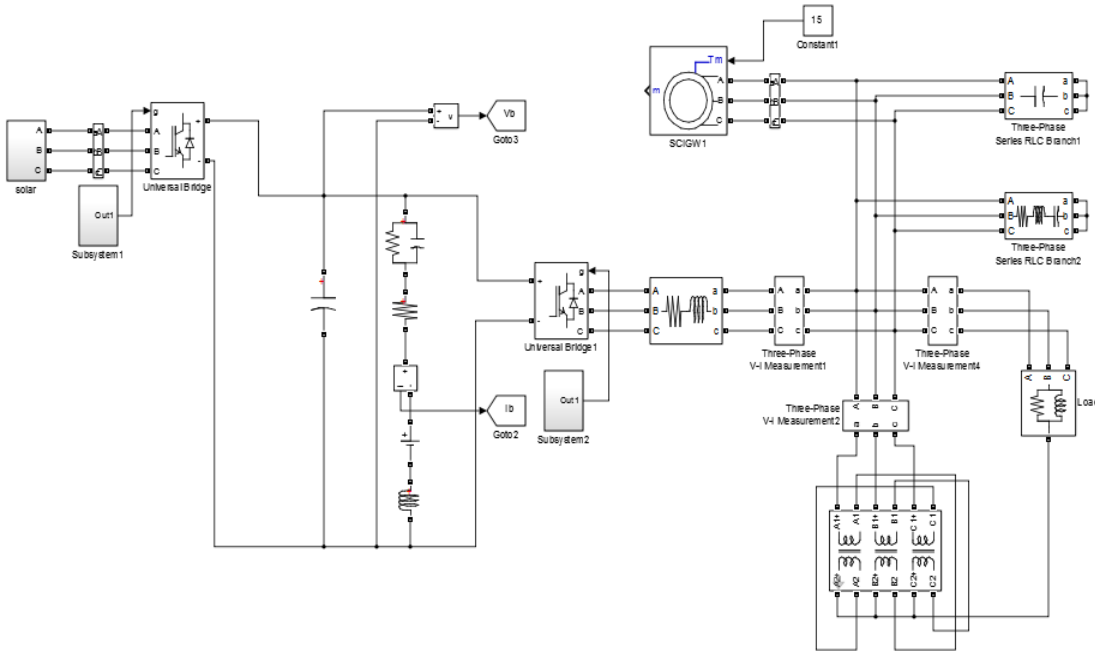


Fig.8. MATLAB simulation diagram of Solar-hydro hybrid system.

a). Performance of Wind-Hydro Hybrid System with Balanced Linear Load

In this case simulation results of wind hydro hybrid system with balance linear load at wind speed (V_w) of 11m/s are shown. Waveforms of corresponding quantities are shown in Fig.9. In

this case rotor speed set point (ω_{rw}) is at 99.6rad/sec it is calculated by using equation (2). Stator frequency(f_w) is 47.08Hz. This frequency theoretically calculated by using equation, $f = (N * P / 120)$. Where N is speed calculated using $N = (\omega * 60 / 2\pi)$ and $\omega = ((2 * \pi * N) / 60)$. Mechanical

power (P_w) corresponding to maximum coefficient of performance at this speed is 52kW. The output power generated by $SCIG_h(P_h)$ is 33.3kw. The total power generated is $(52+33.3)$ kW=85.3kW. Load connected to system is three single phase loads each of (20kW and 10kvar) per phase. The active load connected per phase is 20kW, so total active load $= (20+20+20)=60$ kW. The power generated by system is 85.3kW which is greater than load connected to system of 60kW so extra power is stored in battery (P_b) to maintain frequency of load voltage constant. Reactive power requirement of load is supplied by load side converter to maintain the load voltage magnitude constant. So in this condition load voltage magnitude (i_{sw}) and (i_{sh}) and frequency (f_L) both are maintained constant. Load current (i_L) is balanced. From result waveforms it is observed wind and hydro generator stator currents (i_{sw}) and (i_{sh}) are stable, also load side converter current i_c is balanced. The Cp is 0.422. The rms value of phase load voltage V_t is 240 volts. Battery voltage Vdc is 700V and battery current shown by (I_b). Power generated by both generators which is 85.3kW out of which 60 kW is consumed by load which is shown by graph P_L . Remaining amount of power $(85.3-60=25.3$ kW) is transferred to battery shown in graph P_b equal to 25.3kW.

b).Performance of Wind-Hydro Hybrid System with Unbalanced Linear Load

In second case simulation results of wind hydro hybrid system with unbalance linear load at wind speed (V_w) of 8m/s are shown. Fig.10. shows waveforms of corresponding quantities. In this case rotor speed set point (ω_{rw}) of wind generator is at 72.45rad/sec and stator frequency (f_w) is 34.17Hz. Mechanical power (P_w) corresponding to maximum coefficient of performance at this speed is 20kw. The output power generated by $SCIG_h(P_h)$ is 33.3kw. The total power generated is $(20+33.3)$ kW=53.3kW. Load connected to system is three single phase loads each of (30kW) per phase. So the total active load is of 90kW. The system is started with electrical balance load of 30kW per phase which is connected between each phase and neutral terminal In this case power generated by system is 53.3kW which is less in amount than total load connected to the system (P_L) of 90kW so battery supplies deficit power.

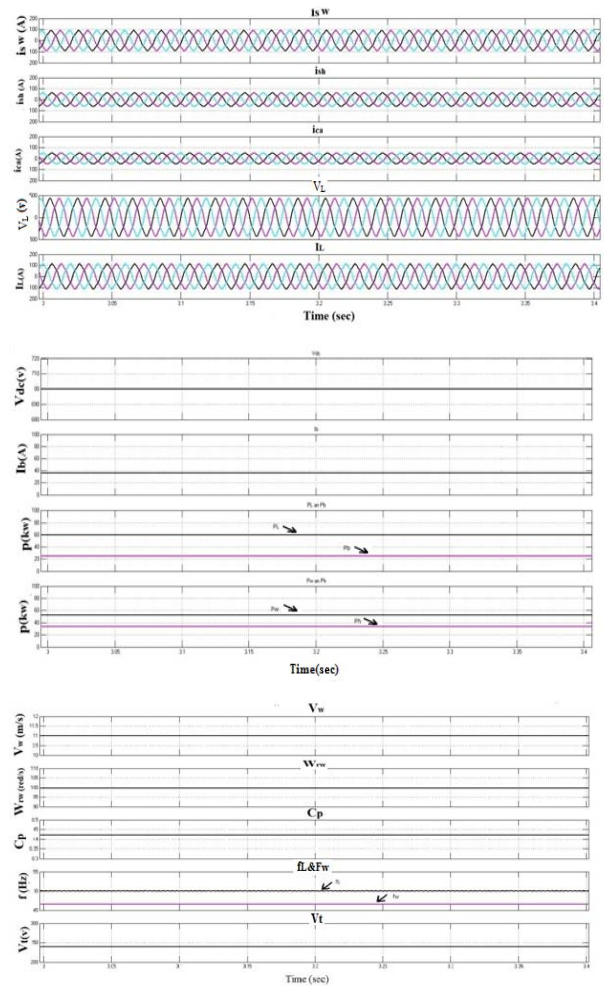


Fig.9. Performance of Wind-Hydro hybrid system with balanced linear load at wind speed of 11 m/s.

At 3.2s, 30kW load from phase “a” is disconnected to create unbalance in system. Now the load on system reduced from 90 to 60 kW and amount of power supplied by battery (P_b) is decreased to maintain load frequency constant. At 3.5s, again load on system is reduced from 60 to 30 kW ie load in phase “b” is disconnected which is of 30kW. At this stage load on system is 30kW only in phase “c” which is less than power generated of 53.3kW, so to maintain frequency of load voltage constant battery absorbs extra power. Reactive power requirement of load is supplied by load side converter to maintain frequency and magnitude of load voltage constant. When linear load is balance the current in zig-zag windings are zero. But during unbalance linear load condition

current in zig-zag windings are nonzero shown by waveforms of (i_{ta} , i_{tb} , i_{tc} , and i_{tn}). After currents in all the three zig-zag windings are same, indicating that zero sequence currents are flowing through these windings. Load currents are shown by waveforms of (i_{La} , i_{Lb} , and i_{Lc}). Current in phase “a” is shown by (i_{La}) this current is zero after 3.2secs as load in this phase is disconnected at 3.2sec. load in phase “b” is disconnected at 3.5sec after this load current is zero in this phase. Load current in phase “c” is shown by i_{Lc} which is continuous. Battery voltage and battery current are shown by (V_{dc}) and (I_b). The rms value of phase load voltage (V_t) is 240 volts.

It is observed that under balance and unbalance linear load conditions, the wind generator and hydro generator stator currents (i_{sw}) and (i_{sh}), and load voltages (v_L) are stable, even load side converter currents (i_c) are balanced. Load voltage magnitude and frequency (f_L) are maintained constant

2) Results for Solar-Hydro Hybrid System

To this PV-Hydro hybrid system balance load of 60kW active and 30 kvar reactive is connected and system performance is observed. Results are shown in fig.11. It is observed that power generated by Solar generation is 46kW for 1000w/m² irradiation and power generated by hydro generation is 33kW so total power generated is (46+33.3)=79.3kW. Active load connected to system is 60kw so load is supplied by hydro power and solar power and remaining amount of power is stored in battery as generated power is greater than load requirement which is of (79.3-60)=19.3kW. At a time we can observe solar and hydro generation currents are balance. Load voltage and frequency are maintained constant.

VII. CONCLUSION

Wind-hydro and solar hydro have ability to complement each other. Two systems are developed for isolated locations. These are three phase four wire autonomous systems. Wind-hydro System performance is observed for balance and unbalance load. Solar-hydro system performance is observed under balance load. Both systems performance satisfactorily having ability of MPT, load balancing and voltage and frequency control of load and filtering zero sequence components of load current.

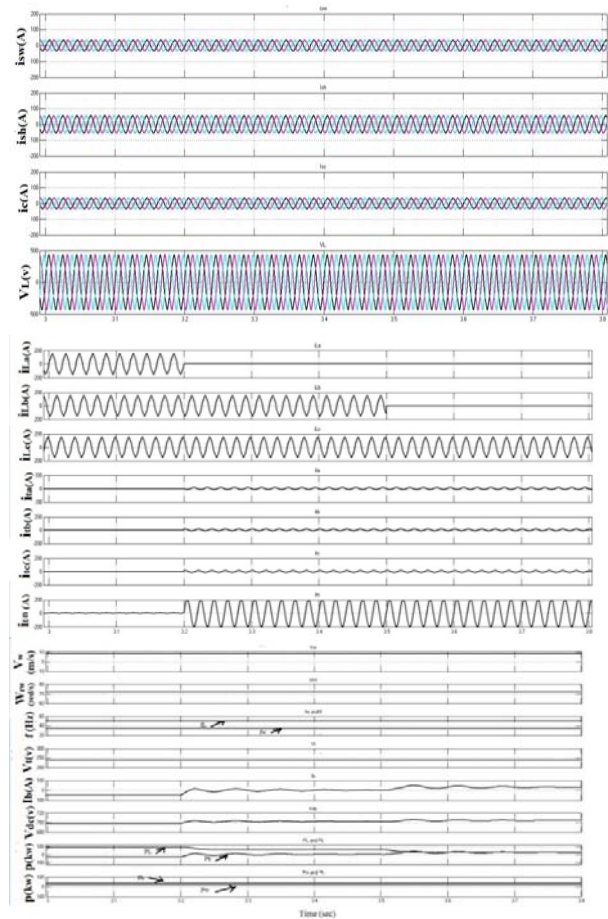


Fig.10. Performance of wind-hydro hybrid system with balanced/ unbalanced linear loads at wind speed of 8 m/s.

APPENDIX

1) Battery Specifications: $C_b = 43.156$ F, $R_b = 10$ k Ω , $R_{in} = 0.2$ Ω , $V_{ocmax} = 750$ V, $V_{ocmin} = 680$ V, Storage= 600kW.h, $L = 1$ mH.

2) Transformer Specification: Three single phase transformers of 15 kVA 138/138 V. connected in zig-zag manner.

3) PI Controllers: Voltage controller: $K_{pv} = 15$ and $K_{iv} = 0.05$.

4) Parameters of 37.3kW 415V 50-Hz Y-connected four-pole SCIG_h: $R_s = 0.09961$ Ω , $L_s = 0.867$ mH, $R_r = 0.058$ Ω , $L_r = 0.867$ mH, $L_m = 0.030369$ H, and Inertia=0.4 kg.m².

5) Parameters of 55-kW wind turbine: wind-speed range = 6.0-11.2 m/s, speed range = 43-81 r/min, $I = 13.5$ kg.m², $r = 7.5$ m, $C_{Pmax} = 0.4412$, and $\lambda^* = 5.66$.

6) Parameters of 55.5kW 415V 50-Hz Y-connected six-pole SCIG_w: $R_s = 0.059$ Ω ,

$L_s=0.687$ mH, $R_r=0.0513$ Ω , $L_r=0.867$ mH,
 $L_m=0.0298$ H, and Inertia=1.5 kg.m².

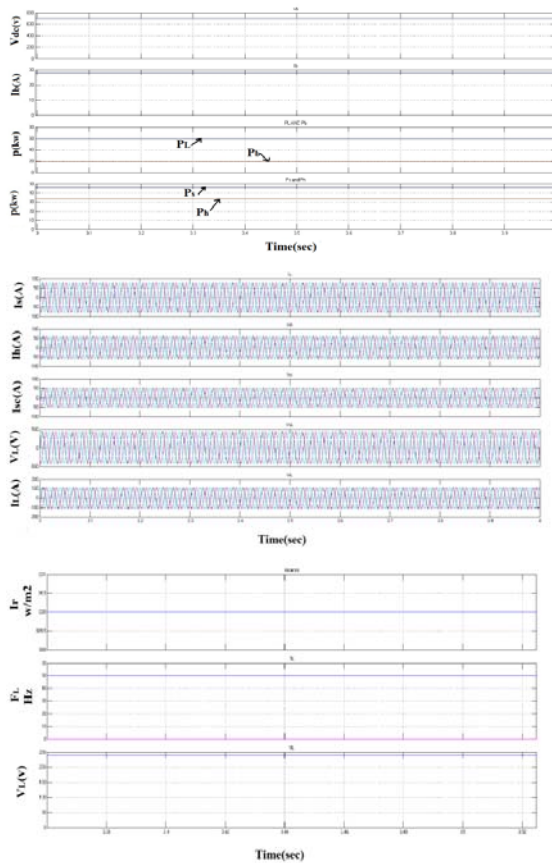


Fig.11.Performance of solar-hydro hybrid system with Balance load.

REFERENCES

- [1] Puneet K. Goel, Bhim Singh, S. S. Murthy, and Navin Kishore, "Isolated Wind-Hydro IEEE Transactions on Industrial, Vol. 58, No. 4, April 2011. Hybrid System Using Cage Generators and Battery Storage,"
- [2] L.-R. Chen, R. C. Hsu, and C.-S. Liu, "A design of a grey-predicted Li-ion battery charge system," IEEE Trans. Ind. Electron, Vol. 55, no. 10, pp. 3692–3701, Oct. 2008.
- [3] M. Black and G. Strbac, "Value of bulk energy storage for managing wind power fluctuations," IEEE Trans. Energy Convers, Vol. 22, no. 1, pp. 197–205, Mar. 2007.
- [4] E. D. Castronuovo and J. A. Pecas, "Bounding active power generation of a wind-hydro power plant," in Proc. 8th Conf. Probabilistic Methods Appl. Power Systems, IA, 2004, pp. 705–710.
- [5] S. Mishra, P. C. Sekhar, "Sliding Mode Based Feedback Linearizing Controller For a PV System to Improve the Performance under Grid Frequency Variation," 2011 IEEE
- [6] B. Singh, S. S. Murthy, and S. Gupta, "An improved electronic load controller for self-excited induction generator in micro-Hydel applications," in Proc. IEEE Annu. Conf. Ind. Electron. Soc, Nov. 2003, Vol. 3, pp. 2741–2746.
- [7] M. Molinas, J. A. Suul, and T. Undeland, "Low voltage ride through of wind farms with cage generators: STATCOM versus SVC," IEEE Trans. Power Electron, Vol. 23, no. 3, pp. 1104–1117, May 2008.
- [8] J. B. Ekanayake, "Induction generators for small hydro schemes," IEEE Power Eng. J, Vol. 16, no. 2, pp. 61–67, 2002.
- [9] S. Ganesh Kumar, S. Abdul Rahman, and G. Uma, "Operation of self-excited induction generator through matrix converter," in Proc. 23rd Annu. IEEE APEC, Feb. 24–28, 2008, pp. 999–1002.
- [10] E. Diaz-Dorado, C. Carrillo, and J. Cidras, "Control algorithm for coordinated reactive power compensation in a wind park," IEEE Trans. Energy Convers, Vol. 23, no. 4, pp. 1064–1072, Dec. 2008.
- [11] G. Quinonez-Varela and A. Cruden, "Modelling and validation of a squirrel cage induction generator wind turbine during connection to the local grid," IET Gener, Transmiss. Distrib, Vol. 2, no. 2, pp. 301–309, Mar. 2008.
- [12] L. Tamas and Z. Szekeley, "Modeling and simulation of an induction drive with application to a small wind turbine generator," in Proc. IEEE Int. Conf. Autom, Quality Test, Robot, May 22–25, 2008, pp. 429–433.
- [13] A. Luna, P. Rodriguez, R. Teodorescu, and F. Blaabjerg, "Low voltage ride through strategies for SCIG wind turbines in distributed power generation systems," in Proc. IEEE Power Electron. Spec. Conf, Jun. 15–19, 2008, pp. 2333–2339.
- [14] M. Elnashar, M. Kazerani, R. ElShatshat, and M. M. A. Salama, "Comparative evaluation of reactive power compensation methods for a standalone wind

energy conversion system,” in Proc. IEEE Power Electron. Spec. Conf, Jun. 15–19, 2008, pp. 4539–4544.

[15] S. S. Murthy, B. Singh, P. K. Goel, and S. K. Tiwari, “A comparative study of fixed speed and variable speed wind energy conversion systems feeding the grid,” in Proc. IEEE PEDS, Nov. 2007, pp. 736–743.

[16] G. Poddar, A. Joseph, and A. K. Unnikrishnan, “Sensorless variable speed controller for existing fixed-speed wind power generator with unity-power-factor operation,” IEEE Trans. Ind. Electron, Vol. 50, no. 5, pp. 1007–1015, Oct. 2003.

[17] M. G. Simoes, B. K. Bose, and R. T. Spiegel, “Fuzzy-logic-based intelligent control of a variable speed cage machine wind generation system,” IEEE Trans. Power Electron, Vol. 12, no. 1, pp. 87–95, Jan. 1997.

[18] D. Joshi, K. S. Sindhu, and M. K. Soni, “Constant voltage constant frequency operation for a self-excited induction generator,” IEEE Trans. Energy Convers, Vol. 21, no. 1, pp. 228–234, Mar. 2006.

[19] L. A. C. Lopes and R. G. Almeida, “Wind-driven induction generator with voltage and frequency regulated by a reduced rating voltage source inverter,” IEEE Trans. Energy Convers, Vol. 21, no. 2, pp. 297–304, Jun. 2006.

[20] B. Singh and G. K. Kasal, “Voltage and frequency controller for a three-phase four-wire autonomous wind energy conversion system,” IEEE Trans. Energy Convers, Vol. 23, no. 2, pp. 505–518, Jun. 2008.

[21] Z. M. Salameh, M. A. Casacca, and W. A. Lynch, “A mathematical model for lead-acid batteries,” IEEE Trans. Energy Convers, vol. 7, no. 1, pp. 93–97, Mar. 1992.

[22] Shridhar Sholapur, K. R. Mohan, T. R. Narsimhegowda, “Boost Converter Topology for PV System with Perturb And Observe MPPT Algorithm” IOSR Journal of Electrical and Electronics Engineering (IOSR-JEEE) e-ISSN: 2278-1676, p-ISSN: 2320-3331, Vol. 9, Issue 4 Ver. II (Jul – Aug. 2014), PP 50-56.

[23] G. Iwanski and W. Koczara, “DFIG-based power generation system with UPS function for variable-speed applications,” IEEE Trans. Ind. Electron, Vol. 55, no. 8, pp. 3047–3054, Aug. 2008.

[24] G. Iwanski and W. Koczara, “Sensorless direct voltage control of the stand-alone slip ring induction generator,” IEEE Trans. Ind. Electron, Vol. 54, no. 2, pp. 1237–1239, Apr. 2007.

[25] Dominguez Garcia, Jose Luis, “Modeling and control of Squirrel Cage Induction Generator with Full Power Converter applied to windmills,” 2009.

[26] [Online]: Available at <http://andaman.nic.in>

[27] J. G. Slootweg, S. W. H. Haan, H. Polinder, and W. L. Kling, “General model for representing variable speed wind turbines in power system dynamics simulations,” IEEE Trans. Power Syst, Vol. 18, no. 1, pp. 144–151, Feb. 2003.

[28] B. K. Bose, “Modern Power Electronics and AC Drives,” Singapore: Pearson Education, Pte. Ltd., 2005, ch. 8.

[29] B. Singh, S. S. Murthy and S. Gupta, “Analysis and design of STATCOM based voltage regulator for self-excited induction generators,” IEEE Trans. Energy Convers, Vol. 19, no. 4, pp. 783–790, Dec. 2004.

[30] Sweeka Meshram, Ganga Agnihotri and Sushma Gupta, “Modelling of grid connected DC linked pv-hydro hybrid system,” An International Journal (ELELIJ), Vol 2, No 3, August 2013.

[31] Sweeka Meshram, Ganga Agnihotri, and Sushma Gupta, “Performance Analysis of Grid Integrated Hydro and Solar Based Hybrid Systems,” Hindawi Publishing Corporation Advances in Power Electronics, Vol 2013, Article ID 697049, 7 pages <http://dx.doi.org/10.1155/2013/697049>